Rotation of a Rectangular Jet by Periodic Excitation

E. Avihar,* N. Shemesh,* and A. Seifert†
Tel-Aviv University, 69978 Ramat-Aviv, Israel
and
L. G. Pack‡
NASA Langley Research Center, Hampton, Virginia 23681

Introduction

CONTROLLED jet rotation is desirable for many engineering applications such as steering, mixing enhancement, increased vehicle maneuverability, safety, and agility. To date, two known methods are used for jet rotation. The first involves using a secondary stream comprising properly placed and directed nozzles. The second method uses turning vanes to interact directly with the jet and force it to rotate. The former method is suitable for fundamental studies but not practical, and the latter method causes thrust loss, requires a heavy mechanism, and is slow to respond, due to large inertial loads. An active method for jet rotation that does not require any moving parts or high-pressure source, because it utilizes zero-mass-flux fluidic actuators, is proposed and demonstrated.

It was shown[1] that periodic excitation can be used to either deflect or enhance the mixing of a circular jet when a short, wide angle diffuser was attached at the jet exit and excitation was introduced at the junction between the jet exit and the diffuser inlet. The reason for the effectiveness of the technique is the enhanced mixing across the separated jet shear layer and the interaction of the latter with the diffuser wall that is promoted by large vortical structures. The presence of the diffuser wall, confining the entrainment of ambient fluid, significantly enhances the jet deflection angle produced by the periodic excitation.[1] The jet deflection angle was shown to be sensitive to the relative direction between the excitation and the jet stream. Excitation with $\langle c_\mu \rangle$ smaller than 0.5% that was introduced in the streamwise direction deflected the jet towards the excited shear layer side, whereas excitation with $\langle c_\mu \rangle$ greater than 0.5% that was introduced in the radial, cross-stream, direction pushed the jet away from the actuator. Recent results[2] demonstrate that the two modes of excitation can be combined to produce jet deflection angles higher than those measured when using a single actuator. When both actuators were operated at identical frequency, the jet deflection angles were sensitive to the relative phase between the actuators, and with proper phase tuning it was always possible to obtain at least the sum of the individual effects.

Method

Rotation of a 3:1 aspect ratio rectangular jet by periodic excitation was demonstrated experimentally. Four piezoelectric actuators were placed around the exit of a 152.4 by 50.8 mm jet. As shown in Fig. 1, a short, wide-angle diffuser was attached at the jet exit, immediately downstream of the excitation slots. The two sidewalls were planar and transparent. Two actuators, covering half of the jet exit width, had their exit slots directed in the streamwise direction, and two actuator exit slots, also covering half of the jet exit width, pointed in the cross-stream direction (Figs. 1a and 1b). Periodic excitation that emanated from the streamwise actuators (X excitation), combined with the diffuser walls, tends to reattach the separated jet shear layers to the diffuser walls (as in flap separation control[3,4] and jet applications[1]). The result of placing two X actuators covering the upper right and lower left halves (76.2-mm) of the long axis shear layers was deflection of the jet flow toward the excitation slot, the left side up and the right side down (looking into the jet, Fig. 1a). Additional jet modification was achieved by the activation of high-amplitude cross-stream excitation (R actuator, Fig. 1) that pushes the jet away from the excitation slot[1,2,5] positioned at the upper left and lower right shear layers. The combination of the four actuators in the current configuration should cause the jet to rotate.

Experimental Setup

The jet facility used for this experiment was a modular assembly of sections designed to allow maximum flexibility in this and future active flow control experiments. The flow was driven by a centrifugal blower feeding a rectangular settling chamber with an entrance cross section 235 mm wide by 286 mm high and exit 336 mm wide by 286 mm high. A honeycomb and screens were installed in the settling chamber, followed by a contraction from circular (entrance diameter $D_{\text{in}} = 303$ mm) to rectangular cross section exit, 50.8 mm high (H) by 152.4 mm wide, resulting in a hydraulic diameter of 76.2 mm. The distance between the duct entrance and the jet exit was 66.7 mm, and a boundary-layer tripping device was not used. The sidewalls of the exit duct are made of acrylic plastic. Short, divergent walls (30-deg inclination) were attached to the long axis of the duct exit, immediately downstream of the excitation slots (Fig. 1b). The length of the diffuser walls, measured from the slot exit to the diffuser exit along the diffuser wall, was 19.05 or 15.45 mm, the longer diffuser downstream of the R-actuator slots (Fig. 1b). Two actuator chambers were situated along each long sidewall of the jet

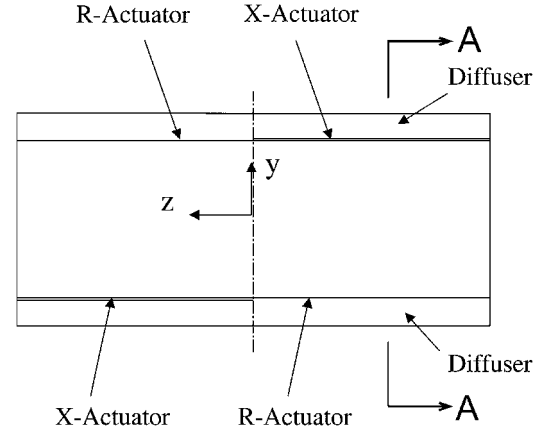

Fig. 1a Front view of the jet exit and actuators; see text for dimensions.

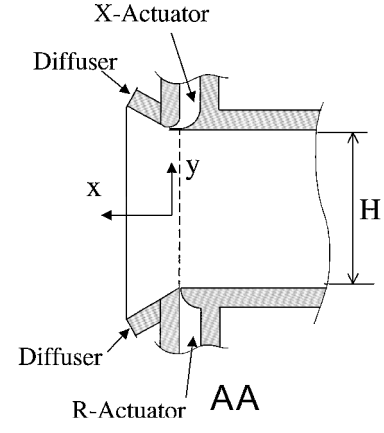

Fig. 1b Side view of the jet exit, diffuser, and actuator slots.

Received 21 July 2002; revision received 22 August 2002; accepted for publication 31 August 2002.

*Research Assistant, Dept. of Mechanics Materials and Systems.
†Senior Lecturer, Department of Fluid Mechanics and Heat Transfer, Faculty of Engineering; Seifert@eng.tau.ac.il. Associate Fellow AIAA.
‡Research Engineer, Flow Physics and Control Branch, Aerodynamics, Aerothermodynamics and Aeroacoustics Competency, Mail Stop 170.

exit duct. The resonance frequency of the R actuators was 700 Hz, and for the X actuators, it was 800 Hz. Each actuator was capable of independent operation, and all actuators were operated at their resonance frequencies, to obtain maximum output. Slot widths were 0.45 mm ± 10%. The slot exit velocities were measured for a range of frequencies and amplitudes, with a hot-wire placed at the slot exit and the jet flow turned off (data acquisition and processing as in Ref. 1). The hot-wire was mounted on a three-dimensional traversing mechanism. The velocity uncertainty was less than 2%.

Figures 2a and 2b present typical results measured at three locations along each of the actuator slots. The variation of the excitation magnitude along each slot was within ±10%. Part of the scatter was due to difficulties in locating the hot wire at the center of the narrow slots where the gradients in the excitation magnitude were very large. The magnitude of the fluctuating slot velocity rms (u'_s) for the entire test was 15 m/s ± 6%.

The definition of the fluctuating momentum injected by the periodic excitation is based on the ratio of the total periodic momentum input and the jet total linear momentum,

$$\langle c_\mu \rangle \equiv (2h/H)(u'_s/U_j)^2$$

where h is the slot width, H the jet height, and U_j is the mean jet exit velocity. The momentum coefficient used throughout this investigation was 0.04 with an uncertainty of ±15%. The preceding definition of the oscillatory momentum coefficient is calculated using a uniform excitation magnitude across the slot width and along its entire length and is, therefore, an upper limit for $\langle c_\mu \rangle$. The mean jet exit velocity was $U_j = 10 \pm 0.5$ m/s, resulting in a Reynolds number (based on hydraulic diameter) of 4.9×10^4.

Flowfield data were acquired using a miniature total pressure probe mounted on the traversing system. Total pressure was measured using a 10-torr pressure transducer (referenced to the ambient pressure, uncertainty of ±0.02% full scale), and the analog output from the transducer was read using a computer interfaced digital multimeter with a resolution of 5.5 digits. A commercial "fog" generator, typically used for theatrical productions, was used to produce a dense white vapor (smoke) for visualizing the jet flowfield. A 6-W argon ion laser powered at 0.5 W was used to generate the light sheet. Still images were acquired at each flow condition and were later digitized, enhanced, and analyzed.

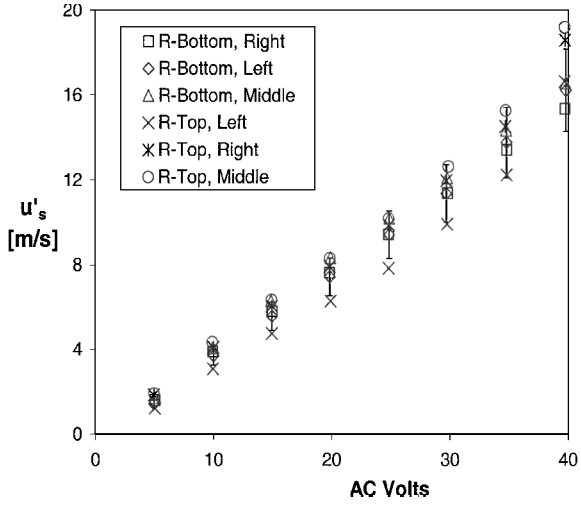

Fig. 2a Calibration of R actuators at 700 Hz; velocity rms in meters per second.

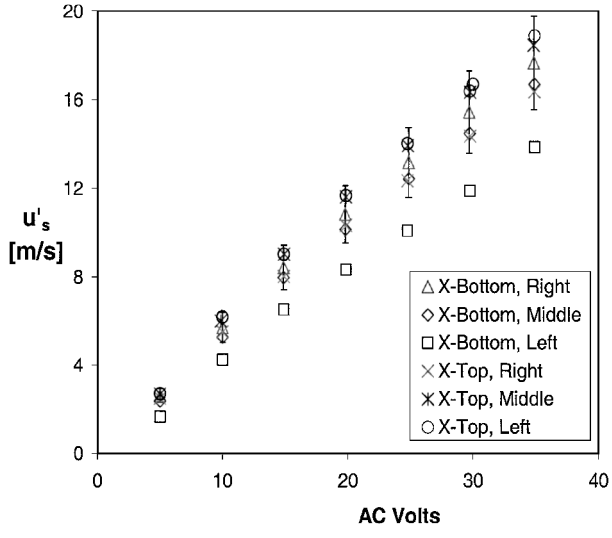

Fig. 2b Calibration of X actuators at 800 Hz; velocity rms in meters per second.

Results

The flow at the jet exit was characterized by a "top hat" velocity profile as measured by the pitot tube (Figs. 3 and 4a) and also seen from the smoke flow visualization picture taken at a distance of 25.4 mm from the jet exit ($x/d_h = 0.33$, not shown). Velocity profiles acquired at several locations along the long axis of the jet at $x = 25.4$ mm indicate very good cross-sectional uniformity. See the baseline profiles in Fig. 3 (filled symbols).

When periodic excitation with a total $\langle c_\mu \rangle \approx 4.0\%$ was applied from the four actuator slots, the velocity profiles (open symbols in Fig. 3) differed significantly from their baseline shape (filled symbols in Fig. 3). At $z = 0$, the jet cross section shrinks in Y; at $z = 38$ mm, the velocity profiles were displaced up; and at $z = -38$ mm, the profiles were displaced down. Because of limits on the travel of the total pressure probe, the $z = 38$ mm data terminate at $y \approx 40$ mm, whereas the $z = -38$ mm data were mirror imaged for illustration. The vertical location of the center of the jet linear streamwise momentum indicates that the profiles were shifted up and down by 10 ± 1 mm from their original y (≈0) location, whereas the shrinking at the center plane indicates spanwise stretching. The combined effect is indicative of jet rotation.

The data in Fig. 4 present baseline and modified velocity contours. These data were acquired at a plane parallel to the jet exit and perpendicular to the main flow direction 25.4 mm from the jet exit. The baseline flow is very close to being a perfect rectangle, in good agreement with the top hat velocity distributions of the baseline data in Fig. 3, whereas the controlled data indicate rotation in the clockwise direction. The small deviations of the baseline velocities from uniformity at the long axis shear layers are attributed to different boundary conditions at the excitation slots. The jet rotation angle was estimated using two independent methods. One method is based on the vertical shift of the center of streamwise linear momentum of each half of the jet (cut at $z = 0$) from the line $y = 0$, based on the data in Fig. 4. The second method is based on the

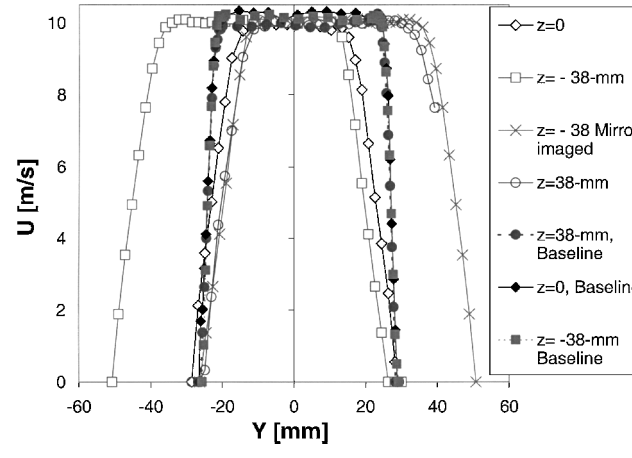

Fig. 3 Mean velocity profiles of baseline and controlled flow at x = 25.4-mm, U = 10 m/s, X and R actuator excitation, and total $\langle c\mu \rangle$ = 4%.

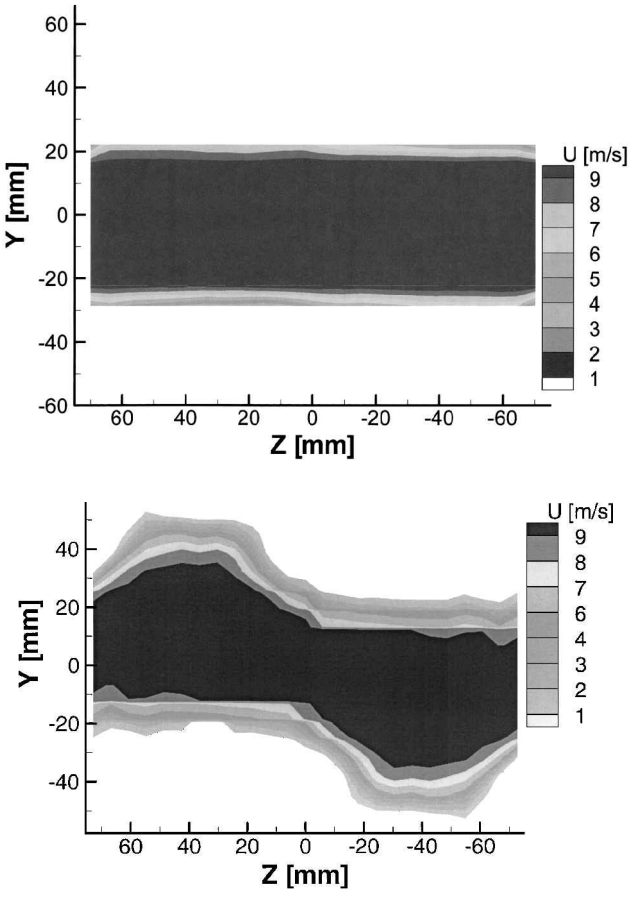

Fig. 4 Mean velocity contours of flow at $x = 25.4$ mm, X and R actuator excitation, $\langle c\mu \rangle = 4\%$: a) baseline flow and b) controlled flow.

identification of the angle generated between the jet principle axis and the Z axis, using the flow visualization pictures (not shown) and taking into account the smoke density, using the 8-bit grayscale resolution. These calculations indicate that the jet was rotated by 13 ± 4 deg at $x/d_h = 0.33$, with respect to the baseline condition.

To verify that the measured data are indicative of jet rotation, and not only modification of the jet velocity distribution at the exit plane, additional flow visualization pictures were acquired at distances of 76.2 and 127.0 mm from the jet exit plane (not shown). The rotational momentum of the free jet should be conserved, so that the observed rotation angle is expected to increase as the observation plane is moved in the streamwise direction. Indeed, the flow visualization images that were acquired farther downstream validate this trend (not shown). The controlled jet data exhibits the same features as the measurements made at $x = 25.4$ mm, but the rotation angle, evaluated using identification of the major axis, is 30 ± 4 deg at $x = 127.0$ mm ($x/d_h = 1.67$), a significant increase with respect to the rotation angle measured at $x = 25.4$ mm. The use of two different excitation frequencies, disregarding the relative phase between the two pairs of actuators is not optimal.

Conclusions

The results clearly demonstrate that a rectangular jet can be rotated using properly placed and directed actuators. The method demonstrated in this Note should allow jet rotation without moving parts, with short-duration transients and in a controlled and gradual manner.

Acknowledgments

The experiment was performed while the first and last authors were visiting ICASE, NASA Langley Research Center. The help and support provided by Richard White and Luther Jenkins are greatly appreciated. Many helpful comments were provided by S. P. Wilkinson, who reviewed the manuscript.

References

[1]Pack, L. G., and Seifert, A., "Periodic Excitation for Jet Vectoring and Enhanced Spreading," *Journal of Aircraft*, June 2001; also AIAA Paper 99-0672, Jan. 1999.

[2]Pack, L. G., and Seifert, A., "Multiple Mode Actuation of a Turbulent Jet," AIAA Paper 01-0735, Jan. 2001.

[3]Seifert, A., Bachar, T., Koss, D., Shepshelovits, M., and Wygnanski, I., "Oscillatory Blowing, a Tool to Delay Boundary Layer Separation," *AIAA Journal*, Vol. 31, No. 11, 1993, pp. 2052–2060.

[4]Seifert, A., Darabi, A., and Wygnanski, I., "Delay of Airfoil Stall by Periodic Excitation," *Journal of Aircraft*, Vol. 33, No. 4, 1996, pp. 691–699.

[5]Smith, B. L., and Glezer, A., "Vectoring and Small-Scale Motions Effected in Free Shear Flows Using Synthetic Jet Actuators," AIAA Paper 97-0213, Jan. 1997.

Side Force on a Rough-Surface Ogive Cylinder: Effects of Freestream Turbulence

K. B. Lua* and S. C. Luo†
National University of Singapore, Singapore 119260, Republic of Singapore
and
E. K. R. Goh‡
Defence Science Organization National Laboratories, Singapore 118230, Republic of Singapore

Nomenclature

A	=	axial distance from model nose tip
b	=	grid bar diameter
C_p	=	pressure coefficient, $(p - p_\infty)/(0.5\rho U_\infty^2)$
C_y	=	side force coefficient, $F_y/(0.5\rho U_\infty^2 S)$
$C_y(A)$	=	local side force coefficient, local side force/$(0.5\rho U_\infty^2 D \sin^2 \alpha)$
$\lvert C_y \rvert$	=	absolute value of the side force coefficient
$\lvert \overline{C_y} \rvert$	=	mean of the absolute value of all of the side force coefficients in the $0 \le \phi < 360$ deg range
D	=	cylinder diameter
d_{particle}	=	average diameter of aluminum oxide particles
F_y	=	side force
I	=	turbulence intensity
I_x	=	longitudinal turbulence intensity in freestream direction, σ_x/U_∞
L	=	turbulence length scale
L_x	=	longitudinal turbulence length scale in the freestream direction
M	=	mesh opening length
P	=	pressure on model surface

Received 24 February 2002; revision received 30 April 2002; accepted for publication 1 May 2002.

*Research Fellow, Department of Mechanical Engineering, 10 Kent Ridge Crescent.

†Associate Professor, Department of Mechanical Engineering, 10 Kent Ridge Crescent.

‡Senior Member of the Technical Staff, Aeronautic Systems Program, 20 Science Park Drive.